Highly Unsaturated Oligomeric Hydrocarbons: α-(Phenylethynyl)-ω-phenylpoly[1,2-phenylene(2,1-ethynediyl)]

Robert H. Grubbs and Detlef Kratz*[+]

California Institute of Technology, Department of Chemistry and Chemical Engineering,
164-30, Pasadena, CA 91125, U.S.A.

Received June 2, 1992

Key Words: Poly[1,2-phenylene(2,1-ethynediyl)], phenyl-capped / Substituted 1,2-Diethynylbenzenes, substituted / π systems, conjugated extended / Oligo(acenes) / Helical structures

A new set of conjugated oligomers $C_6H_5C{\equiv}C-(1,2\text{-}C_6H_4C{\equiv}C)_n-C_6H_5$ (**10**; $n = 3-7$) comprised of acetylene and phenyl units linked together at the 1,2 positions of the aromatic ring is introduced. The facile synthesis of these compounds is achieved through the Pd-mediated coupling reaction of diiodo- and dibromobenzene with the appropriate ethynyl component. Spectroscopic data of the new compounds are discussed in light of electronic conjugation of the extended π system. Thermolysis of oligomers **10** indicates that rearrangement of the triple bonds occurs to form higher conjugated oligo(acenes). The topology of two members (**10**; $n = 2, 3$) is confirmed by X-ray analysis and reveals a propensity for intramolecular π-stacking of the phenyl rings leading to a helical arrangement.

Introduction

Phenylene-acetylene polymers of general formula **10** have received very little attention to date. While compounds with a *meta* or *para* substitution pattern at the benzene ring have been reported[1,2], to our knowledge, a 1,2 linkage to form *acyclic* oligo- or poly(phenylene-acetylenes) (Scheme 1) have not been synthesized. *Cyclic* (i.e. **2**) analogues like those reported by Sondheimer[3a], Staab[3b], Eglington[3c] and Kloster-Jensen[3d] on the other hand are well-known, and similar yet extended systems are obtained when the triple bond is

Scheme 1. Some known (**1**–**4**) and new (**5**–**9**) phenyl-capped poly[1,2-phenylene(2,1-ethynediyl)] compounds

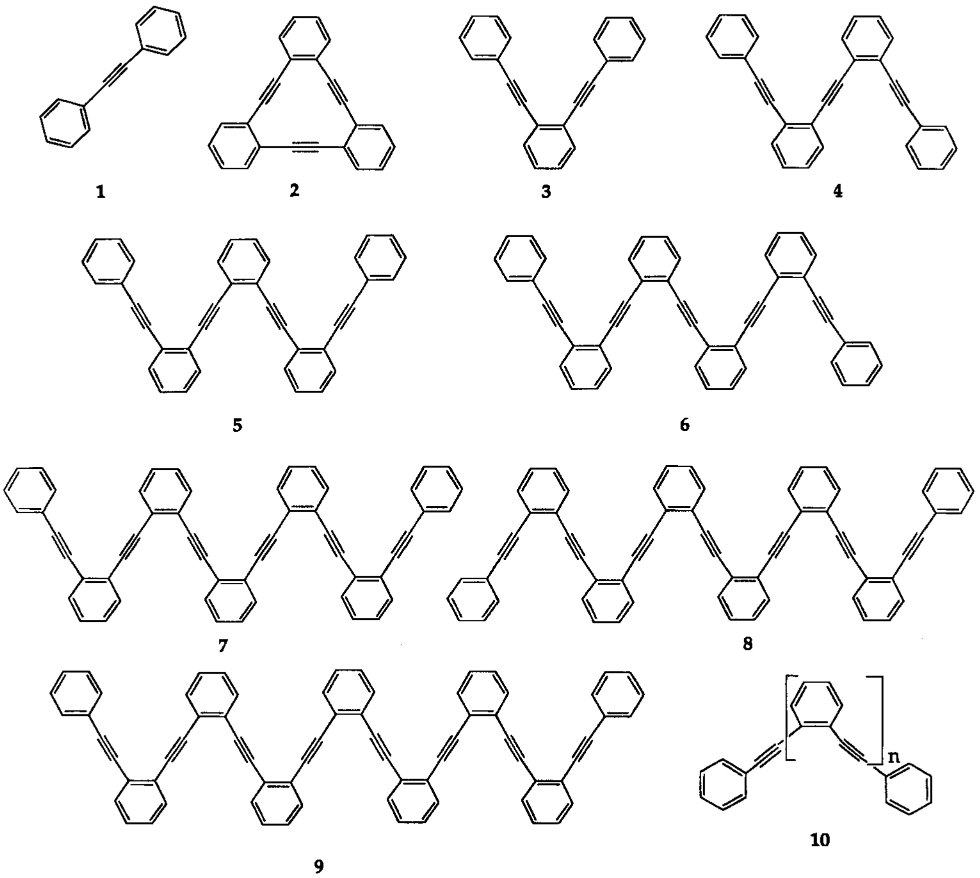

[+] New address: Organisch-Chemisches Institut der Universität, Im Neuenheimer Feld 270, W-6900 Heidelberg, F.R.G.

replaced by the equally linear 1,3-diacetylene moiety[4–6]. More recently a dendrimer built up of a *meta*-connected phenylene-acetylene wedge has been reported by Moore and Xu[7].

Our interest in these systems stems from observations related to the topology of the alternating π units in **10**, and a number of reasons made these oligomers an attractive synthetic goal:

(1) If one considers the geometry of the 1,2-disubstituted ethynyl-aryl moiety, it becomes apparent that the two triple bonds are at a distance which will enable a cyclization process to take place. Ring closure can proceed at the C atoms nearest or farthest to each other to furnish an annulated six-membered[8] (naphthalene **II**) or four-membered[9] (benzocyclobutane **III**) ring, respectively (Scheme 2). A five-membered ring[10,11] (fulvene **IV**) is obtained when cyclization occurs diagonally with respect to the reacting triple bonds.

Scheme 2. Possible ring-closing reactions of 1,2-disubstituted ethynylbenzenes

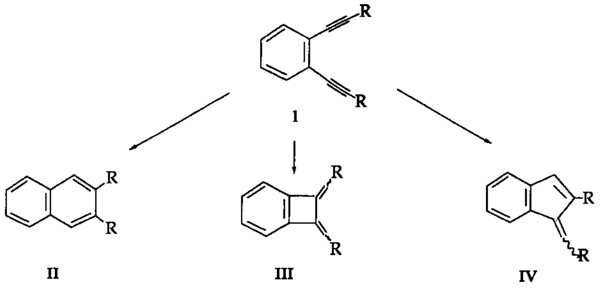

The aim of this study was to multiply the above cyclization steps[12] to achieve the one-step formation of annulated, conjugated arenes by domino-type folding of the closely spaced acetylenic units to yield one-dimensional conductors in the form of graphite-like strands[13]. Compounds such as **5–9** are ideally suited for this purpose as they show high C/H ratios. The outlined conversion step can also be compared to the polymerization of acetylene to poly(acetylene), yet in the described case polymerization occurs "within" a polymer leading to "poly(acetylene)" embedded in a matrix of benzene rings. Short segments of possible reaction products are depicted in Scheme 3.

Scheme 3. Segments of poly(acenes) from **5–9**

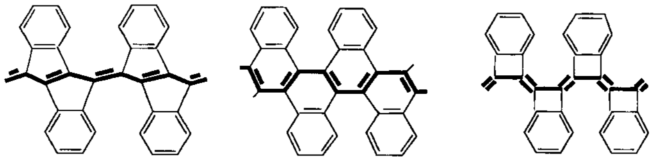

(2) Oligomers **5–9** are not only valuable as precursors for multiple cyclization steps, but are of interest in their own right. In contrast to the rigid and therefore intractable 1,4-connected analogues, the topology determined by 1,2 substitution will lead to higher flexibility and allow not only inter- but also intramolecular stacking of the benzene rings to occur. This is achieved by simple rotation about the sp-sp^2 linkages leading to a helical arrangement.

(3) Finally, **5–9** are linear, conjugated systems which makes them good model compounds for the study of optical and electroactive phenomena that are sometimes difficult to measure in the high molecular weight polymers due to insufficient solubility and intractability[14]. These properties may further be "tuned" by functionalization or derivatization (i.e. variation of the 1,2-phenyl units, hydrogenation of the triple bonds) of **10**.

Synthesis

A number of routes can be designed to obtain the compounds depicted in Scheme 1. After initial experiments adopting step-growth polymerization similar to the work reported by Marvel[1] and an approach using metathesis of 1,2-diethynyl compounds[15], we opted for a step-by-step synthesis.

This strategy utilizes the well-documented Pd-mediated coupling of terminal acetylenes to aryl halides as the essential building step[16,17]. The necessary components are trimethylsilylacetylene (**13**) as a means of introducing a monoprotected triple bond and 1,2-dibromo- (**11**) or 1,2-diiodobenzene (**12**) to achieve the desired *o* connectivity. The reaction sequence outlined for the synthesis of **5–9** in Scheme 4 is straightforward.

All coupling reactions were carried out in a standard procedure by using triethylamine as solvent and $Pd[P(Ph)_3]_4$ (3 mol-%)/CuI (5 mol-%) as catalyst. Reaction of 1,2-dibromobenzene (**11**) with trimethylsilylacetylene (**13**) led to 1-bromo-2-trimethylsilylethynylbenzene (**14**). Subsequent coupling of **14** with phenylacetylene (**15**) afforded 1-phenyl-2-[2-(trimethylsilylethynyl)phenyl]acetylene (**16**) in good yield. At this stage in the reaction sequence other endcapping groups may easily be introduced simply by varying the terminal acetylene used in this step. Cleavage of the trimethylsilyl protecting group was achieved by stirring **16** with KF in DMF[16] to give **17** (this form of deprotection was also used in all subsequent steps). When **17** was treated with 0.8 equiv. of **12** two products, the monoadduct **18** (35%) and the oligomer **5** (54%), were formed.

Separation was carried out by flash chromatography on SiO_2. Compound **18** was converted (into **19**) by treatment with **13** using the outlined Pd-coupling conditions and then deprotected with KF to give **20**, the next higher phenylethynyl analogue of **17**, in 88% yield.

To obtain the oligomers with an even number of aryl groups, the ethynyl component (**20** or **23**) was treated with the respective iodo component (**18** or **21**) in a 1:1 ratio to form the oligomers **6** or **8** in 74 and 82% yield, respectively. The oligomers with an uneven number of phenyl groups (**5**, **7** and **9**) were produced in the addition step of the ethynyl-substituted compounds (**17**, **20** and **23**) with 1,2-diiodobenzene (**12**), along with the next higher iodo compound (**18**, **21** and **24**) necessary for the subsequent steps. This strategy allows for variation of the π system by exchanging **12** with other 1,2-dihalo compounds at this point (i.e. heterocycles, donor- or acceptor-substituted benzenes or quinoid units).

Scheme 4. Synthetic route to oligomers 5–9

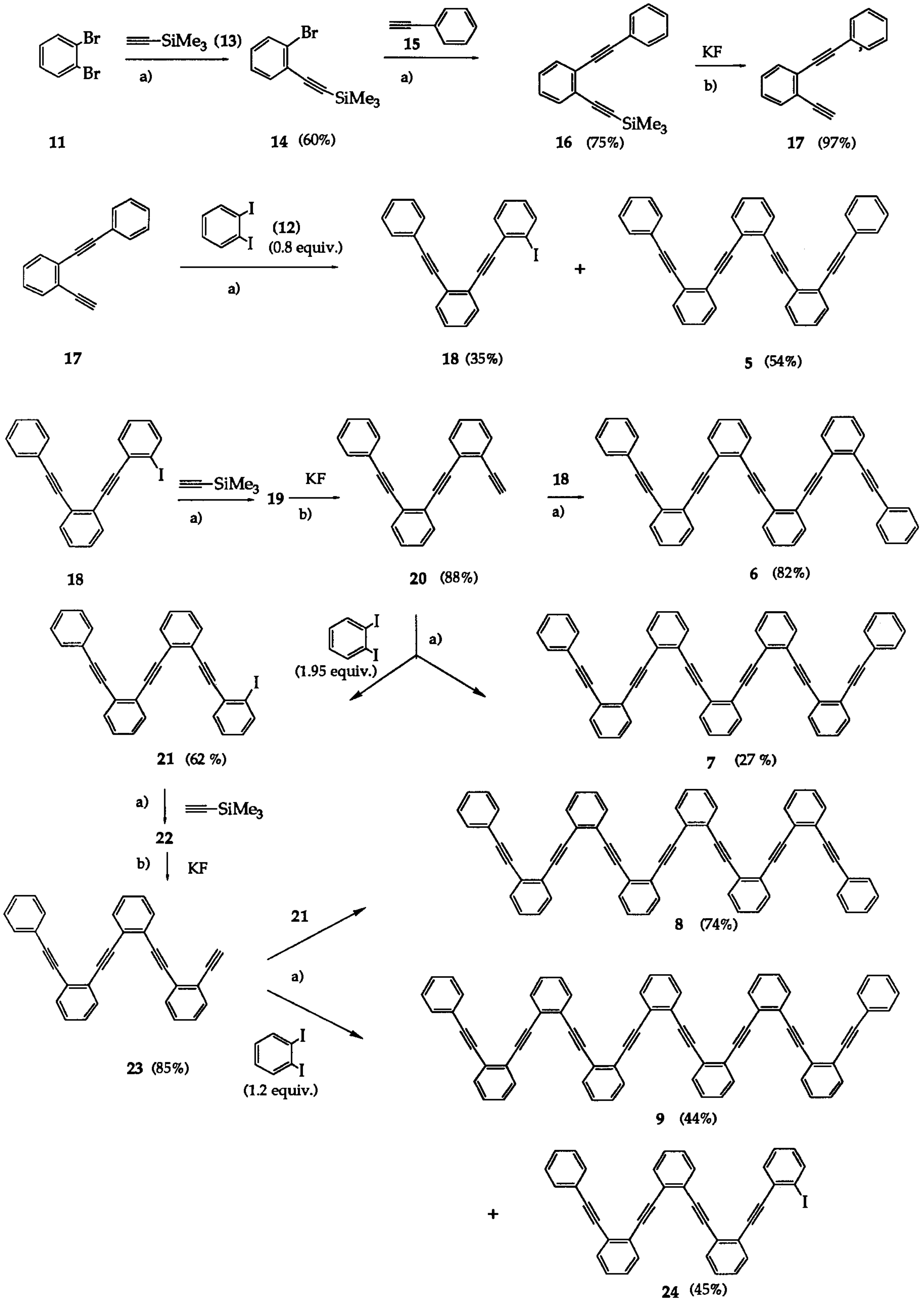

a) Pd[P(Ph)$_3$]$_4$ (3 mol-%)/CuI (5 mol-%) in triethylamine, reflux. – b) KF, DMF/H$_2$O, 20°C.

All products were purified by column chromatography, which was especially facile since **5**−**9** fluoresce intensely (vide infra) on long-wavelength irradiation and can be detected on the column.

To complete the set of oligomers for the sake of comparison of the spectroscopic characteristics that are discussed below, **2**[17], **3**[16] and **4**[10] were prepared according to literature procedures.

Spectroscopic Properties

All oligomers are white to slightly tan solids that dissolve well in benzene and CH_2Cl_2 and may be recrystallized from hot ethanol. On crystallization they show a pronounced tendency to form thin flaky wafers. The mass of **5**−**9** as measured by high-resolution (FAB) mass spectrometry agrees with the calculated values.

The ^1H-NMR spectra (see Table 1) show a strong overlap of the signals of the aromatic protons. The ^{13}C-NMR spectra, on the other hand, are more useful with respect to identification of the obtained structures. Especially the region between $\delta = 75$ and 95, typical for the acetylene resonance signal, usually allows the determination of the number of triple bonds. As is to be expected the sp-hybridized C atoms tend to give signals lying at very similar chemical shifts as the chain grows longer, and the expected number of signals is not always reflected in the spectrum. The same observation is made for the aromatic region which shows three separate clusters of signals. From comparison with data from the literature[18] the following assignments are made. The resonance lines at $\delta \approx 131$ are due to the *o*-carbon atoms, the second set at $\delta \approx 128$ reflects the absorption of the *m*- and *p*-carbon atoms and the signals at $\delta \approx 125$ can be assigned to the quaternary carbon atoms. One single resonance is found at $\delta \approx 123$ which arises from the *p*-carbon atom of the end-capping phenyl group. Neither the ^1H-NMR nor the ^{13}C-NMR spectra show any pronounced effects that are indicative of a helical structure in solution.

The IR spectra of **3**−**9** are very similar, the most pronounced bands occurring at $\tilde{\nu} \approx 3000$, 1400−1600, 1200 and between 690 and 740 cm^{-1} (see Table 1). The spectrum is dominated by bands of the aromatic rings, and the acetylene stretching vibration is very weak and sometimes cannot be observed at all.

With this series of oligomers in hand it was interesting to examine the effect of chain length (**10**; $n = 0-7$) on the extent of conjugation. An excellent and simple tool to gauge the amount of electronic delocalization is by UV/Vis and fluorescence spectroscopy. In addition, the values observed on electrochemical oxidation or reduction will give valuable information in the assessment of the relative HOMO and LUMO energies. The most pertinent data of **1**−**9** are collected in Table 1.

Table 1. Characteristic spectroscopic data of **1**−**9**

Compound	**1**	**2**	**3**	**4**	**5**	**6**	**7**	**8**	**9**
^1H NMR in CD_2Cl_2 δ [ppm] (#H)	7.4 (8), 7.62 (6)	6.66 (6), 7.18 (6)	7.35 (2), 7.37 (6), 7.58 (8)	7.31 (2), 7.35 (6), 7.53 (4), 7.61 (4)	7.26 (2), 7.31 (8), 7.36 (2), 7.55 (8), 7.64 (2)	7.26 (2), 7.30 (2), 7.54 (6), 7.59 (6)	7.22 (2), 7.29 (14), 7.52 (8), 7.39 (6)	7.22(4), 7.29 (14), 7.55 (16)	7.20 (8), 7.29 (12), 7.54 (18)
E_{Ox} [V]	-	-	-	+2.25	+2.01	+1.95	+1.90	+1.855	+1.84
UV/VIS in Ethanol λ_{max} [nm] (log ε)	216 (4.28), 220 (4.23), 264 (4.31), 278 (4.47), 287 (4.32), 298 (4.25) to 303	263 (4.54), 270 (4.96), 278 (4.92), 287 (5.36), 319 (3.63), 330 (3.64) 342 (3.80)	221 (4.36), 247 (4.32), 259 (4.50), 272 (4.68), 311 (4.29), 330 (3.90) to 340	217 (4.55), 252 (4.59), 265 (4.78), 277 (4.57), 292 (4.47), 316 (4.31) to 356	252 (4.50), 265 (4.66), 303 (4.29) to 364	217 (4.84), 250 (4.77), 266 (4.88) 313 (4.60) to 371	265 (4.94), 302 (4.62) to 376	265 (4.87), 303 (4.61) to 384	265 (4.91), 315 (4.54) to 388
Fluorescence in Ethanol λ_{max} [nm]	299, 313, 319 to 380	355, 372, 427, 452, 475, 490, 515, 545	onset 323, 342, 356, 364 to 464	onset 335, 356, 372, 384 to 480	onset 337, 357, 373, 384 to 486	onset 338, 368, 386 to 506	onset 342, 372, 389 to 516	onset 345, 377, 392 to 529	onset 347, 382 to 543
DSC [°C]: endoth.	61	213	48	91	120	141	121	142	134
exoth. (kJ/mol)	207 (endoth.)	317 (114.3)	320 (99.8)	306 (336.7)	299 (486.1)	292 (506.9)	292 (570.8)	284 (597.5)	286 (519.7)
HRMS [m/z]					478.1712	578.2014	678.2334	778.2610	878.2930
IR [cm^{-1}] in CH_2Cl_2	3081, 2299, 2218, 1601, 1572, 1497, 1442, 1265, 766, 711, 690	3053, 2216, 1605, 1488, 1438, 1276, 805, 730, 671	3052, 2304, 2215, 1755, 1599, 1495, 1442, 1259, 770, 732, 689	3045, 2216, 1599, 1495, 1444, 1271, 1257, 766, 724, 707	3065, 2334, 2217, 1961, 1598, 1495, 1445, 1263, 768, 692, 678	3054, 2216, 1598, 1495, 1446, 1270, 766, 724, 706, 689	3054, 2961, 2213, 1605, 1495, 1422, 1269, 768, 726, 687	3055, 2962, 1604, 1496, 1272, 767, 723, 707, 688	3054, 2213, 2297, 1598, 1495, 1447, 1271, 769, 725, 707, 688

The results reflect the influence of increasing chain length nicely, and **9** with a total of 70 conjugated π-electron units exhibits the most pronounced red shift of its UV absorption. The long-wavelength absorption does not show a large extinction coefficient but rather tails off with maximum absorption reaching λ = 388 nm in **9**. This is reflected on a qualitative basis with the lack of color in all compounds. Overall, the excitation spectra are nicely complimented by the fluorescence spectra which show a symmetric relationship in appearance to the former and exhibit an equally gradual shift of the lowest energy transition towards longer wavelengths. The data collected for **2** should be viewed separately, as the cyclic system introduces other factors[3a,c] (in fact, **2** is pale yellow because of three weak absorptions between λ = 320 and 340 nm). Most characteristic is the pronounced increase of the lowest energy transition ($S_0 \rightarrow S_1$ or $S_1 \rightarrow S_0$) in the excitation and emission spectra of the shorter compounds. Continuing along the series to **9** does not have such a marked effect, and the shift of λ drops from an initial step of Δλ = 27 nm (**1** → **3**) and Δλ = 16 nm (**3** → **4**) to an average of Δλ = 6.2 nm (**4** → **9**) in the UV/Vis absorption spectra. The long-wavelength feature of the spectra is observed as a broad band that may be assigned to overlap of the π orbitals of the phenyl and acetylene units. The tailing of this band probably arises due to rotation of the phenyl-ethynyl moieties out of the molecular plane which decreases overlap of the p orbitals. The increasing chain length of oligomers **4**–**9** and subsequent rise in vibrational motion is also reflected in the excitation spectra. Whereas the spectra of **4** and **5** still exhibit distinct vibrational bands, the line shapes for **6**–**9** are featureless.

The electronic spectra give an indication of the decreasing energy gap of these systems. Analysis of the redox potentials will give information as to the relative shift of the HOMO and LUMO to higher or lower energies. CV spectra of **1** and **3**–**9** were measured in CH_2Cl_2 by using a glassy carbon electrode, tetrabutylammonium tetrafluoroborate as added electrolyte and are referenced to SCE by calibration with ferrocene[19]. None of the compounds show a tendency for reduction within the measured range. An oxidation wave is first observed for **4** at $E = +2.25$ V. The lowest potential was monitored for **9** ($E = +1.84$ V), the difference between the oxidation maxima falling from $\Delta E = 0.24$ V (**4** → **5**) to $\Delta E = 0.05$ V on going from **8** to **9**. It can be expected that greater chain lengths (**10**; $n > 7$) will not lead to significantly higher potentials. This limiting effect is similar to the decrease in λ shifts noted above, and from these facts it may be inferred that the number of conjugated units is limited to only a few phenyleneacetylene moieties as vibration of the molecular framework as well as rotation about the sp-sp^2 linkage will drastically reduce delocalization. Alternatively, it is to be expected that charge is mainly localized at each adjoining unit, and the small effects observed with increasing number of n are a result of minor disturbances which perturb the localized system. Variation of the building blocks, by introducing other benzenoid rings during synthesis or by selective reduction of the triple bonds to yield 1,2-substituted oligo(phenylene-vinylenes) is a possible way of increasing delocalization[20].

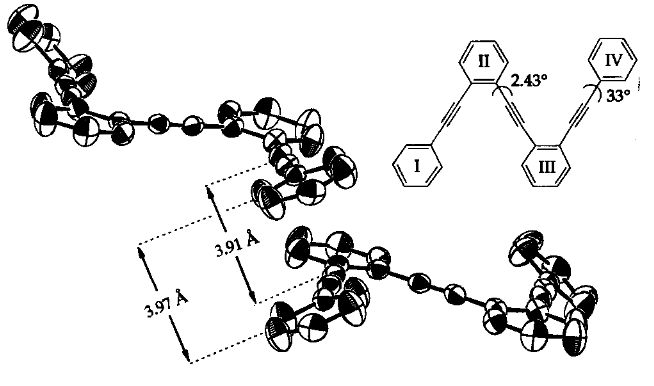

Figure 1. Sideview of two molecules of **4** in the unit cell

All of the oxidations exhibit the characteristic wave form of an irreversible process. Continuing positive cycles eliminate the oxidation maximum completely, and after ten cycles a slightly red, shiny film is deposited on the electrode surface. On scanning towards negative voltage ($E = -1.8$ V) after deposition no reduction was observed.

Structures of 4 and 5

From the spectroscopic analysis above no clear indication of the molecular geometry of 1,2-substituted phenylene-acetylenes could be derived. To obtain an impression of the structural characteristics of this class of compounds an X-ray analysis was performed on single crystals of oligomers **4** and **5** (Figure 1 and 2)[21]. The salient features of these results are outlined below.

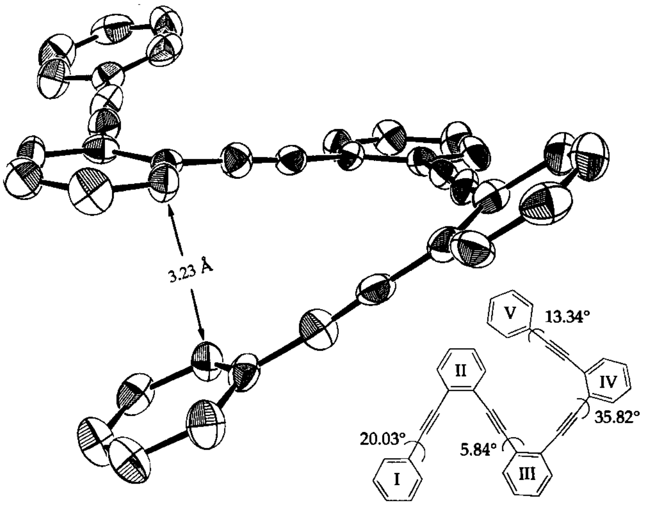

Figure 2. View of the helical conformation of **5**

In **4**, the three triple bonds define a nearly perfect plane of the molecule with the two central phenyl moieties (II, III) twisted only by 2.43° relative to each other. The end-capping phenyl groups (I, IV), on the other hand, are rotated appreciably out of the plane of the molecular framework. This twist occurs in opposing directions and amounts to an interplanar angle with respect to the central plane of 33°. The measured bond angles and bond lengths are not out of the ordinary, the distance between the triple bonds lies between 2.90 Å and 4.24 Å, which is closely related to the values observed in **2**[22].

The unit cell of **4** is more complex. Four individual units are observed, and closer scrutiny of molecular packing in the cell reveals good alignment (π stacking) of every "outer" diphenylacetylene unit (see Figure 1). The intermolecular distances reach values of 3.85 and 3.98 Å for the triple bonds and range between 3.84 and 4.07 Å or 4.21 and 4.55 Å for the respective aromatic rings. Obviously, effects caused by packing of the molecules are very important in the solid state, and the fact that a fairly flat structure is revealed may be attributed to strong π-π interactions.

The structure of **5** shows some relationship to that of **4**, in that three triple bonds form a fairly planar arrangement (rings II and III are twisted by 5.89° relative to each other). The adjoining phenyl rings (I, IV) are twisted out of this plane as in **4** (20.03° and 35.82°, respectively), yet this rotation occurs in the same direction. The most interesting feature is the position of the final phenylethynyl moiety. Instead of facing away from the central part of the molecule to form an elongated geometry as drawn in the formula representation in Scheme 1, the preferred conformation in the solid state is one in which this unit folds back onto the second benzene ring. Although the two rings (II and V) are not perfectly aligned the short intramolecular distances (between 3.23 Å and 3.77 Å) indicate that in addition to packing forces, favorable π-π interaction may be the cause of stacking leading to the observed helical topology. These results are also in line with the spectroscopic data which reveal that rotation about the sp-sp^2 bonds is facile allowing for helical orientation of the phenylethynyl moieties.

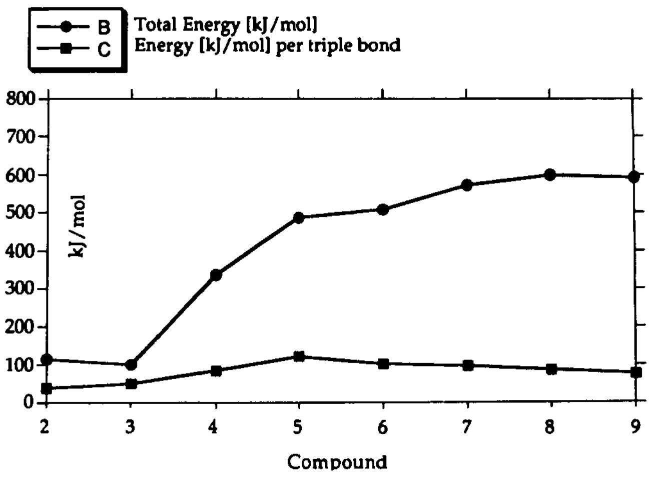

Figure 3. Normalized DSC traces of **3**–**9** (from top to bottom)

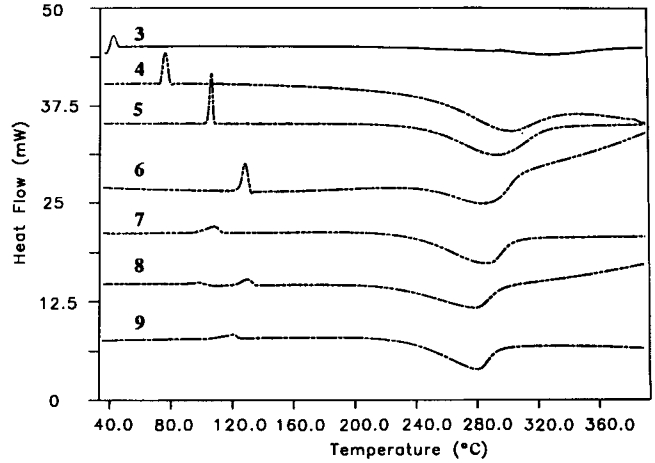

Figure 4. Energy output on thermolysis of **2**–**9**

Thermal Properties of 1–9

To ascertain the reactivity of the 1,2-diethynyl units on heating, the thermal properties of **1**–**9** were investigated by means of differential scanning calorimetry (DSC). The data in Figure 3 reveals that all compounds with a 1,2-substitution pattern behave similarly on heating. The endothermic process at lower temperature is a sharp peak for the *acyclic* lower molecular weight compounds (**1**, **3**–**6**) while this feature becomes broad and decreases in temperature for the longer chains (**7**–**9**). Presumably the chains with $n > 4$ do not melt but rather exhibit a conformational rearrangement at this temperature. The most important aspect of these curves is the clear-cut exothermic dip at temperatures ranging from 286°C (**9**) to 317°C (**3**) which may reflect a cyclization process as mentioned in the introduction. Even the cyclic trimer **2** behaves similarly and after melting at 213°C goes through this exothermic process. In an attempt to induce thermal [2 + 2 + 2] cycloaddition of the three triple bonds in **2**, Staab and co-workers[3c] had heated **2** at 240°C for 30 min and were able to retreive the starting material in almost quantitative yield. The DSC trace clearly shows that temperatures in excess of 300°C are required for thermal rearrangement to take place. Only the monoacetylene **1** does not fit into the picture; instead of an exothermic process it shows a slight endothermic rise at 207°C after initially melting at 61°C.

One of the advantages of DSC is that the consumed or evolved amount of energy can be calculated by integration of the area of the registered peak. The amount of heat evolved from the exothermic process rises steeply from 100 kJ/mol (**3**) to 500 kJ/mol in **5** and then only slowly climbs further to 590 kJ/mol for **8** and **9** (Figure 4). The large values monitored in these measurements make a radical process very likely. Reaction may be initiated by a cyclization process as pointed out in Scheme 2 to produce a biradical species that can then polymerize the triple bonds either in an inter- or intramolecular manner.

Figure 4 also includes a plot of the calibrated data where each value has been divided by the number of triple bonds per molecule. Thus, thermolysis of **5** gives rise to the largest amount of evolved energy per triple bond (121.5 kJ/mol). On scanning the thermolyzed samples a second time no exo- or endothermic features are registered which indicates that an irreversible process is taking place.

Polymerization of these compounds may, of course, be induced chemically (either cationically, anionically or radically) or by transition-metal catalysis. Some preliminary results on reaction of **5** with electrophiles such as Br_2, as well as the metal complexes $PdCl_2$, $PtCl_4$ and $CpCo(CO)_2$ have shown promising results. Further research aimed at analyzing the structural, spectroscopical and chemical aspects of these interesting precursors will show whether this approach to poly(acenes) is feasable.

The authors acknowledge the support of the *Alexander-von-Humboldt Foundation* (D.K.) and the *AFOSR* for support of this research.

Experimental

General Procedures: All work involving air- and/or moisture-sensitive compounds was performed by using standard high-vacuum (10^{-5} Torr) or Schlenk techniques under argon (not purified) and a Vacuum Atmospheres drybox under nitrogen. – ^1H and ^{13}C NMR: Bruker AM 500 and Oxford QE 300 operating at 500.137, 300.102 and 75.468 MHz, respectively. Chemical shifts were referenced to residual protio solvents. – GC: Hewlett-Packard Model 5890 (series II) coupled to a Hewlett-Packard 5970 Series Mass Selection Detector. – Electrochemical experiments were performed in a nitrogen-filled dry box by using a PAR-179 potentiostat and PAR-175 programmer. – Voltammetry was performed by using a 3-electrode configuration in a 1-compartment cell. The non-aqueous reference electrode was Ag/Ag^+, and potentials were referenced to SCE by calibration with the Fe/Fe^+ couple of ferrocene (420 mV versus SCE). – DSC was performed with a Perkin-Elmer DSC-7. – Fluorescence spectra were recorded with an SLM 8000 C instrument, the UV/Vis spectra with a Hewlett-Packard 8254 Diode Array instrument. – Flash chromatography was carried out on Merck silica gel (particle size 0.040–0.063 mm, 230–400 mesh ASTM).

Materials: For the syntheses of nonsensitive organic materials, solvents were used without purification. Benzene, toluene, diethyl ether and THF as well as C_6D_6 and $[D_8]THF$ were stirred over sodium benzophenone ketyl and distilled under argon into solvent flasks equipped with a Teflon screw-type valve. Triethylamine was heated over KOH at reflux and distilled under argon.

Synthesis of **5**–**9**. – *General Procedure for Pd-Coupling of Terminal Acetylenes with Aryl Halides:* The aromatic halide was dissolved in triethylamine and heated at reflux temperature under Ar for 45 min. The reaction was allowed to cool to 50 °C, 3 mol-% of $Pd[P(Ph)_3]_4$ and 5 mol-% of CuI were added and stirring was continued at 70 °C for a further 45 min. The terminal acetylene was added by syringe (solids were first dissolved in a minimal amount of degassed triethylamine). On heating a precipitate formed and the reaction turned yellow to brown and sometimes green. The reaction was monitored by TLC, and after the starting compounds had disappeared the mixture was allowed to cool to room temperature.

Table 2. Reaction conditions for the synthesis of **5**–**9** and **14**–**24**

Reaction components	Product (yield in %)	Triethylamine	Solvent for Chromatography
11 8g (34mmol) **13** 3.45g (35mmol)	**14** 5.16g (60%)	250 ml	Petroleumether (PE)
14 2.3g (8.7mmol) **15** 1.45g (15mmol)	**16** 1.78g (75%)	75 ml	Petroleumether
12 3.68g (14.5mmol) **17** 4.8g (8mmol)	**18** 2.54g (35%) **5** 2.35g (54%)	100 ml	PE/CCl_4 10:1 PE/CCl_4 1:1
18 2.25g (5.57mmol) **13** 0.82g (8.35mmol)	**19** 2.1g (98%)	75 ml	CCl_4
18 0.31g (0.76mmol) **20** 0.23g (0.76mmol)	**6** 360mg (83%)	10 ml	CCl_4
12 2.6g (7.8mmol) **20** 3.45g (4mmol)	**21** 1.23g (62%) **7** 370mg (27%)	100 ml	CCl_4 CH_2Cl_2/CCl_4 1:10
21 0.98g (1.95mmol) **13** 300mg (3mmol)	**22** 903mg (97%)	20 ml	CCl_4
21 0.21g (0.42mmol) **23** 0.17g (0.41mmol)	**8** 240mg (74%)	10 ml	CH_2Cl_2/CCl_4 1:10
12 389mg (1.2mmol) **23** 390mg (0.97mmol)	**24** 264mg (45%) **9** 196mg (45%)	25 ml	CH_2Cl_2/CCl_4 1:10 CH_2Cl_2/CCl_4 1:5

Diethyl ether was added and the solid removed by filtration under suction through a frit. After washing the ammonium salt thoroughly with diethyl ether, the solvents were removed, and the brown residue was chromatographed on silica gel with the appropriate solvent (Table 2). Due to the pronounced fluorescence of **5**–**9** on long-wavelength irradiation (λ = 360 nm) detection on the column was possible. The oligomers were obtained as yellow to light brown oils that on addition of *n*-pentane gave white to tan flakes if left to stand at room temperature. The solid was filtered and washed with *n*-pentane. Recrystallization was carried out from hot ethanol. Single crystals of **4** were obtained from *n*-pentane, those of **5** from ethanol. Table 2 summarizes the parameters for the reactions outlined in Scheme 4.

Procedure for Desilylation of **16**, **19** *and* **22**[17]: The protected acetylene compound was dissolved in a mixture of DMF/H_2O (15:1). While stirring at room temperature 1.5 equiv. of KF was added. The mixture was stirred for 3 h and then diluted with water to form a white suspension. After extraction with CH_2Cl_2 (5 ×) and subsequent washing of the combined organic phases with H_2O (4 ×), the organic solution was dried with $MgSO_4$. Finally, after the solvent had been removed, the terminal acetylene was purified by column filtration on SiO_2 by using either petroleum ether or CCl_4 as eluent. The obtained yields were nearly quantitative.

Spectroscopic Data

Diphenylethyne (**1**): M.p. 61 °C (DSC). – ^1H NMR (CD_2Cl_2, 500.1 MHz): δ = 7.4 (m, 6H), 7.62 (m, 4H). – ^{13}C NMR (CD_2Cl_2, 75.4 MHz): δ = 89.6, 123.5, 128.7, 128.8, 131.9. – GC/MS (EI), *m/z* (%): 178 (100), 152 (10), 126 (4), 102 (2), 89 (4), 76 (6). – IR (CH_2Cl_2): $\tilde{\nu}$ = 3081 cm^{-1} (s), 2299 (vw), 1601 (m), 1572 (m), 1497 (m), 1442 (m), 1265 (s), 766 (s), 711 (s), 690 (s). – UV/Vis (Ethanol): λ_{max} (lg ε) = 201 nm (4.70), 216 (4.28), 220 (4.23), 264 (4.31), 278 (4.47), 287 (4.32), 298 (4.25) to 303. – DSC: 61 °C (endothermic), 207 °C (endothermic).

1,2:5,6:9,10-Tribenzocyclododeca-1,5,9-triene-3,7,11-triyne (**2**): M.p. 213 °C (DSC). – ^1H NMR (CD_2Cl_2, 500.1 MHz): δ = 6.66 (q, 6H), 7.18 (q, 6H). – ^{13}C NMR (CD_2Cl_2, 75.4 MHz): δ = 93.0, 126.8, 129.1, 132.4. – GC/MS (EI), *m/z* (%): 278 (100), 276 (70), 250 (5), 200 (1.5), 174 (0.6), 138 (9), 125 (4), 87 (4). – IR (CH_2Cl_2): $\tilde{\nu}$ = 3053 cm^{-1} (s), 2216 (vw), 1605 (m), 1488 (m), 1438 (m), 1276 (s), 805 (s), 730 (s), 671 (s). – UV/Vis (Ethanol): λ_{max} (lg ε) = 201 nm (4.70), 257 (4.36), 263 (4.54), 270 (4.96), 278 (4.92), 287 (5.36), 319 (3.63), 330 (3.64), 342 (3.80). – DSC: 213 °C (endothermic), 317 °C (exothermic).

1,2-Bis(phenylethynyl)benzene (**3**): M.p. 48 °C (DSC). – ^1H NMR (CD_2Cl_2, 500.1 MHz): δ = 7.35 (m, 2H), 7.37 (m, 6H), 7.58 (m, 6H). – ^{13}C NMR (CD_2Cl_2, 75.4 MHz): δ = 88.1, 93.4, 123.1, 125.6, 128.2, 128.4, 128.5, 131.6, 131.8. – GC/MS (EI), *m/z* (%): 378 (100). – IR (CH_2Cl_2): $\tilde{\nu}$ = 3052 cm^{-1} (s), 2304 (vw), 2215 (vw), 1755 (m), 1599 (m), 1495 (m), 1442 (m), 1295 (s), 770 (s), 732 (s), 689 (s). – UV/Vis (Ethanol): λ_{max} (lg ε) = 201 nm (4.70), 221 (4.36), 239 (4.25), 247 (4.32), 259 (4.50), 272 (4.68), 311 (4.29) to 340. – DSC: 48 °C (endothermic), 320 °C (exothermic).

α-Phenylethynyl-ω-phenylbis[1,2-phenylene(2,1-ethynediyl)] (**4**): M.p. 91.3 °C (DSC). – ^1H NMR (CD_2Cl_2, 500.1 MHz): δ = 7.31 (m, 6H), 7.37 (m, 4H), 7.53 (m, 4H), 7.61 (m, 4H). – ^{13}C NMR (CD_2Cl_2, 75.4 MHz): δ = 88.3, 92.3, 93.9, 123.3, 125.8, 125.9, 128.4, 128.5, 128.6, 128.6, 131.8, 132.1, 132.3. – GC/MS (EI), *m/z* (%): 378 (100), 377 (63), 376 (97), 374 (44), 301 (11), 300 (20), 200 (19), 188 (24), 187 (39). – IR (CH_2Cl_2): $\tilde{\nu}$ = 3054 cm^{-1} (s), 2216 (vw), 1599 (m), 1495 (m), 1444 (m), 1271 (s), 1257 (s), 1097 (w), 1026 (w), 895 (w), 766 (s), 724 (s), 707 (s). – UV/Vis (Ethanol): λ_{max} (lg ε) = 201 nm (4.70), 217 (4.55), 252 (4.59), 265 (4.78), 277 (4.57), 292 (4.47), 316 (4.31)–356. – CV (CH_2Cl_2): *E* = +2.25 V (irrev.). – DSC: 91.3 °C (endothermic), 306 °C (exothermic).

α-Phenylethynyl-ω-phenyltris[1,2-phenylene(2,1-ethynediyl)] (**5**): M.p. 120 °C (DSC). – ^1H NMR (CD_2Cl_2, 500.1 MHz): δ = 7.26 (m, 2H), 7.31 (m, 8H), 7.36 (m, 2H), 7.55 (m, 8H), 7.64 (m, 2H). – ^{13}C NMR (CD_2Cl_2, 75.4 MHz): δ = 88.32, 92.28, 92.56, 93.76, 123.3, 125.7, 125.8 (× 2), 128.2, 128.4, 128.5, 128.5, 128.6, 131.8, 131.9, 132.3, 132.4. – HR MS (FAB), *m/z*: 478.1712. – IR (CH_2Cl_2): $\tilde{\nu}$ = 3056 cm^{-1} (s), 2976 (w), 2334 (vw), 2217 (vw), 1961 (vw), 1598 (m), 1495 (s), 1445 (m), 1284 (w), 1263 (s), 1099 (w), 1069 (w), 1031 (w), 951 (w), 916 (w), 768 (s), 722 (s), 692 (s), 678 (s). – UV/Vis (Ethanol): λ_{max} (lg ε) = 202 nm (4.63), 252 (sh, 4.50), 265 (4.66), 303 (4.29)–364. – CV (CH_2Cl_2): *E* = +2.01 V (irrev.), +2.16 (grows in). – DSC: 120 °C (endothermic), 299.9 °C (exothermic).

α-Phenylethynyl-ω-phenyltetrakis[1,2-phenylene(2,1-ethynediyl)] (**6**): M.p. 141.5 °C (DSC). – ^1H NMR (CD_2Cl_2, 500.1 MHz): δ = 7.26 (m, 2H), 7.30 (m, 12H), 7.54 (m, 6H), 7.59 (m, 6H). – ^{13}C NMR (CD_2Cl_2, 75.4 MHz): δ = 88.6, 92.5, 92.7 (× 2), 93.9, 123.4, 125.8, 125.9 (br.), 128.4, 128.6 (× 2), 128.6 (× 2), 128.7, 131.9, 132.1, 132.2, 132.3, 132.4. – HR MS (FAB), *m/z*: 578.2014. – IR (CH_2Cl_2): $\tilde{\nu}$ = 3054 cm^{-1} (s), 2216 (vw), 1598 (m), 1495 (m), 1446 (m), 1270 (s), 1099 (w), 1035 (w), 951 (w), 766 (s), 724 (s), 706 (s), 689 (m). – UV/Vis (Ethanol): λ_{max} (lg ε) = 202 nm (5.01), 217 (sh, 4.84), 250 (sh, 4.77), 266 (4.88), 313 (4.60)–371. – CV (CH_2Cl_2): *E* = +1.95 V (irrev.). – DSC: 141.5 °C (endothermic), 292.9 °C (exothermic).

α-Phenylethynyl-ω-phenylpentakis[1,2-phenylene(2,1-ethynediyl)] (**7**): ^1H NMR (CD_2Cl_2, 500.1 MHz): δ = 7.22 (m, 2H), 7.29 (m, 14H), 7.52 (m, 8H), 7.59 (m, 6H). – ^{13}C NMR (CD_2Cl_2, 75.4 MHz): δ = 88.6, 92.6, 92.7 (× 2), 92.8, 93.9, 123.3, 125.7 (br.), 125.7 (br.), 128.2, 128.3, 128.4, 128.5, 128.6, 128.7, 131.8, 131.9, 132.1, 132.3, 132.4, 132.5. – HR MS (FAB), *m/z*: 678.2334. – IR (CH_2Cl_2): $\tilde{\nu}$ = 3054 cm^{-1} (s), 2961 (w), 2213 (vw), 1605 (m), 1495 (m), 1422 (m), 1269 (s), 1095 (m), 1014 (m), 806 (m), 768 (s), 726 (s), 687 (m). – UV/Vis (Ethanol): λ_{max} (lg ε) = 200 nm (5.14), 265 (4.94), 302 (4.62)–376. – CV (CH_2Cl_2): *E* = +1.90 V (irrev.). – DSC: 121.3 °C (endothermic, br.), 292 °C (exothermic).

α-Phenylethynyl-ω-phenylhexakis[1,2-phenylene(2,1-ethynedyil)] (**8**): ^1H NMR (CD_2Cl_2, 500.1 MHz): δ = 7.22 (m, 4H), 7.29 (m, 14H), 7.55 (m, 16H). – ^{13}C NMR (CD_2Cl_2, 75.4 MHz): δ = 88.5, 92.5, 92.6 (× 2), 92.6, 92.8, 93.8, 123.5, 125.8, 125.9 (br.), 128.4, 128.4, 128.5, 128.5, 128.6, 128.7, 128.8, 131.9, 132.1, 132.1, 132.2, 132.2, 132.3, 132.5, 132.6. – HR MS (FAB), *m/z*: 778.2610. – IR (CH_2Cl_2): $\tilde{\nu}$ = 3055 cm^{-1} (s), 2962 (w), 1604 (m), 1496 (m), 1421 (m), 1272 (s), 1259 (s), 1097 (m), 1013 (m), 896 (w), 807 (m), 767 (s), 723 (s), 707 (s), 688 (m). – UV/Vis (Ethanol): λ_{max} (lg ε) = 202 nm (5.08), 265 (4.94), 302 (4.62)–384. – CV (CH_2Cl_2): *E* = +1.855 V (irrev.). – DSC: 112 °C (endothermic, br.), 142.3 °C (endothermic, br.), 284.6 °C (exothermic).

α-Phenylethynyl-ω-phenylheptakis[1,2-phenylene(2,1-ethynediyl)] (**9**): ^1H NMR (CD_2Cl_2, 500.1 MHz): δ = 7.20 (m, 8H), 7.29 (m, 12H), 7.54 (m, 18H). – ^{13}C NMR (CD_2Cl_2, 75.4 MHz): δ = 88.6, 92.6 (× 2), 92.7 (× 2), 92.8, 92.9, 93.9, 123.5, 125.8, 125.8, 125.9 (br.), 128.4, 128.5, 128.5, 128.6, 128.6, 128.7, 128.8, 131.9, 132.1, 132.4, 132.5 (br.), 132.6. – HR MS (FAB), *m/z*: 878.2930. – IR (CH_2Cl_2): $\tilde{\nu}$ = 3054 cm^{-1} (s), 2980 (w), 2297 (vw), 2213 (vw), 1598 (m), 1495 (m), 1447 (m), 1422 (w), 1271 (s), 1099 (w), 895 (w), 769 (s), 725 (s), 707 (s), 688 (m). – UV/Vis (Ethanol): λ_{max} (lg ε) = 201 nm (5.06), 265 (4.91), 315 (4.54)–388. – CV (CH_2Cl_2): *E* = +1.84 V (irrev.). – DSC: 134.1 °C (endothermic, br.), 286 °C (exothermic).

1-Phenyl-2-[2-(trimethylsilylethynyl)phenyl]ethyne (**16**): ^1H NMR (CD_2Cl_2, 300.1 MHz): δ = 0.03 (s, 9H), 7.3 (m, H), 7.38 (m, H), 7.55

(m, H). – ^{13}C NMR (CD_2Cl_2, 75.4 MHz): δ = 88.2, 93.5, 98.8, 103.4, 123.2, 125.7, 126.0, 128.2, 128.5, 128.6, 128.7, 131.8, 131.9, 132.4. – GC/MS (EI), *m/z* (%): 274 (66), 259 (100), 243 (15), 215 (35), 130 (18), 43 (22).

1-(2-Ethynylphenyl)-2-phenylethyne (**17**): ^{1}H NMR (CD_2Cl_2, 300.1 MHz): δ = 3.46 (s, 1H), 7.33 (m, 5H), 7.6 (m, 4H). – ^{13}C NMR (CD_2Cl_2, 75.4 MHz): δ = 81.3, 82.2, 87.9, 93.5, 123.1, 124.6, 126.3, 128.3, 128.6, 128.8, 128.9, 131.8, 131.9, 132.7. – GC/MS (EI), *m/z* (%): 202 (100), 201 (28), 200 (34), 176 (5), 150 (5), 100 (6), 88 (7), 74 (6).

α-(2-Iodophenyl)-ω-phenylethynyl[1,2-phenylene(2,1-ethynediyl)] (**18**): ^{1}H NMR (CD_2Cl_2, 300.1 MHz): δ = 7.07 (dt, 1H), 7.38 (m, 6H), 7.59 (m, 5H), 7.69 (m, 1H), 7.93 (m, 1H). – ^{13}C NMR (CD_2Cl_2, 75.4 MHz): δ = 88.3, 91.8, 93.7, 95.3, 123.3, 125.3, 125.6, 128.1, 128.4, 128.5, 128.6, 128.7, 128.9, 129.0, 129.3, 131.8, 131.9, 132.0, 132.3, 132.4, 133.0, 139.0. – GC/MS (EI), *m/z* (%): 404 (100), 276 (74), 248 (5), 130 (16).

α-Phenylethynyl-ω-(2-trimethylsilylethynylphenyl)[1,2-phenylene(2,1-ethynediyl)] (**19**): GC/MS (EI), *m/z* (%): 374 (51), 359 (95), 357 (97), 343 (54), 331 (20), 315 (100), 281 (11), 171 (10), 73 (12).

α-(2-Ethynylphenyl)-ω-phenylethynyl[1,2-phenylene(2,1-ethynediyl)] (**20**): ^{1}H NMR (CD_2Cl_2, 300.1 MHz): δ = 3.38 (s, 1H), 7.36 (m, 7H), 7.6 (m, 6H). – ^{13}C NMR (CD_2Cl_2, 75.4 MHz): δ = 81.6, 82.0, 88.2, 91.9, 92.2, 93.7, 123.3, 124.5, 125.5, 125.7, 126.6, 128.3, 128.5, 128.5, 128.6, 128.7, 128.8, 131.9, 132.1, 132.3, 132.5, 132.8. – GC/MS (EI), *m/z* (%): 304 (100), 150 (17), 138 (9).

α-(2-Iodophenyl)-ω-phenylethynylbis[1,2-phenylene(2,1-ethynediyl)] (**21**): ^{1}H NMR (CD_2Cl_2, 300.1 MHz): δ = 7.03 (dt, 1H), 7.31 (dt, 1H), 7.37 (m, 8H), 7.6 (m, 8H), 7.87 (dt, 1H). – ^{13}C NMR (CD_2Cl_2, 75.4 MHz): δ = 88.5, 91.9, 92.5, 92.6, 94.1, 95.7, 101.0, 123.3, 125.5, 125.7, 125.9, 126.0, 128.1, 128.4, 128.5, 128.6, 128.7, 128.8, 128.8, 129.9, 131.9, 132.1, 132.2, 132.6, 132.6, 132.6, 133.2, 138.9.

α-(2-Ethynylphenyl)-ω-phenylethynylbis[1,2-phenylene(2,1-ethynediyl)] (**23**): ^{1}H NMR (CD_2Cl_2, 300.1 MHz): δ = 3.38 (s, 1H), 7.36 (m, 9H), 7.6 (m, 8H). – ^{13}C NMR (CD_2Cl_2, 75.4 MHz): δ = 81.5, 82.0, 88.2, 92.0, 92.1, 92.2, 92.3, 93.8, 123.1, 124.5, 125.5, 125.6, 125.7, 125.8, 126.1, 128.1, 128.3, 128.4, 128.5, 128.5, 128.6, 128.6, 131.7, 131.9, 132.3, 132.4, 132.5, 132.6.

α-(2-Iodophenyl)-ω-phenylethynyltris[1,2-phenylene(2,1-ethynediyl)] (**24**): ^{1}H NMR (CD_2Cl_2, 300.1 MHz): δ = 7.0 (dt, 1H), 7.33 (m, 12H), 7.56 (m, 5H), 7.68 (m, 2H), 7.86 (dt, 1H). – ^{13}C NMR (CD_2Cl_2, 75.4 MHz): δ = 88.6, 92.0, 92.6, 92.7, 92.8, 94.0, 95.7, 101.0, 123.4, 125.5, 125.7, 125.8, 125.9, 125.9, 126.1, 128.1, 128.3, 128.6, 128.7, 128.7, 128.8, 129.9, 130.0, 131.9, 132.1, 132.5, 132.5, 132.7, 132.7, 133.2, 139.0.

---

[1] D. L. Trumbo, C. S. Marvel, *J. Polym. Sci., Part A: Polym. Sci.* **1986**, *24*, 2311–2326.

[2] K. Sanechika, T. Yamamoto, A. Yamamoto, *Bull. Chem. Soc. Jpn.* **1984**, *57*, 752–755.

[3] [3a] R. Wolovsky, F. Sondheimer, P. J. Garratt, I. C. Calder, *J. Am. Chem. Soc.* **1965**, *87*, 5720–5727. – [3b] I. D. Campbell, G. Eglington, W. Henderson, R. A. Raphael, *Chem. Commun.* **1966**, 87–89. – [3c] H. A. Staab, F. Graf, *Chem. Ber.* **1970**, *103*, 1107–1118. – [3d] E. Kloster-Jensen, J. Wirz, *Angew. Chem.* **1973**, *85*, 723; *Angew. Chem. Int. Ed. Engl.* **1973**, *12*, 671.

[4] O. M. Behr, G. Eglington, A. R. Galbraith, R. A. Raphael, *J. Chem. Soc.* **1966**, 3614–3625.

[5] A. S. Hay, *J. Org. Chem.* **1960**, *25*, 1275–1276.

[6] T. X. Neenan, G. M. Whitesides, *J. Org. Chem.* **1988**, *53*, 2489–2496.

[7] J. S. Moore, Z. Xu, *Polym. Prepr. (Am. Chem. Soc., Div. Polym. Chem.)* **1991**, *32*, 629–630; J. S. Moore, Z. Xu, *Macromolecules* **1991**, *24*, 5893–5894.

[8] R. R. Jones, R. G. Bergman, *J. Am. Chem. Soc.* **1972**, *94*, 660–661.

[9] R. Dierks, K. P. C. Vollhardt, *Angew. Chem.* **1986**, *98*, 268–270; *Angew. Chem. Int. Ed. Engl.* **1986**, *25*, 266–268.

[10] H. W. Whitlock, Jr., P. E. Sandvick, *J. Am. Chem. Soc.* **1966**, *88*, 4525–4526; H. W. Whitlock, Jr., P. E. Sandvick, L. E. Overman, P. B. Reichardt, *J. Org. Chem.* **1969**, *34*, 879–886; B. J. Whitlock, H. W. Whitlock, *ibid.* **1972**, *37*, 3559–3561.

[11] E. Müller, H.-G. Fritz, K. Munk, H. Straub, H. Geisel, *Tetrahedron Lett.* **1969**, 5167–5170; E. Müller, J. Heiß, M. Sauerbier, *Liebigs Ann. Chem.* **1969**, *723*, 61–75; E. Müller, K. Munk, P. Ziemek, M. Sauerbier, *ibid.* **1968**, *713*, 40–48.

[12] K. N. Bharucha, R. M. Marsh, R. E. Minto, R. G. Bergman, *J. Am. Chem. Soc.* **1992**, *114*, 3120–3121.

[13] H. Blome, E. Clar, C. Grundmann, *Methoden Org. Chem. (Houben-Weyl)*, 4. Aufl., **1981**, vol. V/2b, p. 359–470.

[14] See: T. A. Skotheim (Ed.), *Handbook of Conducting Polymers*, Vol. 1 and 2, Marcel Dekker, **1986**; J. L. Brédas, R. R. Chance (Eds.), "Conjugated Polymeric Materials: Opportunities in Electronics Optoelectronics and Molecular Electronics", *NATO ASI Ser., Ser. E* **1990**, *182*, and ref. therein; J. Messier, F. Kajzar, P. Prasad, D. Ulrich (Eds.), "Nonlinear Effects in Organic Polymers", *NATO ASI Ser., Ser. E* **1989**, *162*, and ref. therein.

[15] R. H. Grubbs, D. Kratz, results to be published.

[16] S. Takahashi, Y. Kuroyama, N. Hagihara, *Synthesis* **1980**, 627–630.

[17] C. Huynh, G. Linstrumelle, *Tetrahedron* **1988**, *44*, 6337–6344, and ref. therein.

[18] C. F. Wilcox, Jr., K. A. Weber, *Tetrahedron* **1985**, *41*, 4425 to 4436.

[19] Thanks to Dr. *T. H. Jozefiak* for help with the electrochemical measurements.

[20] F. Wudl, S. Bitler, *J. Am. Chem. Soc.* **1986**, *108*, 4685–4687.

[21] R. Marsch, L. M. Henling, D. Kratz, results to be published in *Acta Crystallogr.*

[22] H. Irngartinger, L. Leiserowitz, G. M. J. Schmidt, *Chem. Ber.* **1970**, *103*, 1119–1131.

[234/92]

CAS Registry Numbers

1: 501-65-5 / **2**: 5385-26-2 / **3**: 13203-60-6 / **4**: 35324-43-7 / **5**: 143192-55-6 / **6**: 143192-56-7 / **7**: 143215-13-8 / **8**: 143192-57-8 / **9**: 143192-58-9 / **11**: 583-53-9 / **12**: 615-42-9 / **13**: 1066-54-2 / **14**: 38274-16-7 / **15**: 536-74-3 / **16**: 143192-59-0 / **17**: 143192-60-3 / **18**: 143192-61-4 / **19**: 143192-62-5 / **20**: 143192-63-6 / **21**: 143192-64-7 / **22**: 143192-65-8 / **23**: 143192-66-9 / **24**: 143192-67-0